



OPEN Transcriptomic signatures of feline chronic gingivostomatitis are influenced by upregulated *IL6*

Santiago Peralta^{1,6,7}✉, Jennifer K. Grenier^{2,7}, Suzin M. Webb¹, Andrew D. Miller³, Ileana C. Miranda⁴ & John S. L. Parker⁵

Feline chronic gingivostomatitis (FCGS) is a relatively common and debilitating disease characterized by bilateral inflammation and ulceration of the caudal oral mucosa, alveolar and buccal mucosa, and varying degrees of periodontal disease. The etiopathogenesis of FCGS remains unresolved. In this study, we performed bulk RNA-seq molecular profiling of affected tissues derived from a cohort of client-owned cats with FCGS compared to tissues from unaffected animals, to identify candidate genes and pathways that can help guide future exploration of novel clinical solutions. We complemented transcriptomic findings with immunohistochemistry and in situ hybridization assays to better understand the biological significance of the results and performed RNA-seq validation of biologically relevant differentially expressed genes using qPCR assays to demonstrate technical reproducibility. Transcriptomic profiles of oral mucosal tissues in cats with FCGS are enriched with immune- and inflammation-related genes and pathways that appear to be largely influenced by *IL6*, and include *NFKB*, *JAK/STAT*, *IL-17* and *IFN* type I and II signaling, offering new opportunities to develop novel clinical applications based on a more rational understanding of the disease.

Feline chronic gingivostomatitis (FCGS) is a debilitating disease characterized by bilateral inflammation and ulceration of the caudal oral mucosa, alveolar and buccal mucosa, and varying degrees of periodontal disease^{1–5}. Clinical manifestations include oral pain, difficulty prehending food, ptyalism, and lack of grooming behavior. General physical examination findings often include poor body condition, mandibular lymphadenopathy, and dehydration. Routine clinicopathological blood test results usually identify hyperglobulinemia⁶; routine histopathological assessment of affected oral tissues consistently shows a predominantly lymphoplasmacytic infiltrate covered by an ulcerated or hyperplastic epithelium⁷.

Treatment options currently available for FCGS include medical (e.g., analgesics, anti-inflammatories, antibiotics) and surgical intervention (i.e., partial- or full-mouth dental extractions)⁸. Medical therapy alone is ineffective in the long term while surgery results in partial or complete remission of some animals^{9,10}. However, surgery is invasive, expensive, and technically complex, and often requires intense postoperative management including aggressive analgesia and nutritional support. Additionally, response to surgery typically takes weeks or months. Moreover, up to 30% of cats appear refractory to surgery and eventually require additional medical therapy that may involve a prolonged course of oral cyclosporine¹¹, intravenous injections of adipose-derived stem cells^{12,13}, and topical or systemic administration of recombinant feline interferon (IFN)-omega^{14,15}, among other options. In general, none of the currently available therapeutic alternatives are based on a mechanistic understanding of the disease and all lack markers that can help guide clinical decisions or predict therapeutic response.

According to a survey among general practitioners, and a retrospective review of medical records in a non-referral institution^{16,17}, the estimated prevalence of FCGS in the general cat population ranges between 0.7 and 12%. Although no breed, sex or age predispositions have been documented, the risk of FCGS is significantly

¹Department of Clinical Sciences, College of Veterinary Medicine, Cornell University, Ithaca, NY 14853, USA. ²Transcriptional Regulation and Expression Facility, Biotechnology Resource Center, Institute of Biotechnology, Cornell University, Ithaca, NY 14853, USA. ³Department of Population Medicine and Diagnostic Sciences, College of Veterinary Medicine, Cornell University, Ithaca, NY 14853, USA. ⁴Laboratory of Comparative Pathology, Memorial Sloan Kettering Cancer Center, Weill Cornell Medical College, and The Rockefeller University, New York, NY 10065, USA. ⁵Department of Microbiology and Immunology, College of Veterinary Medicine, Cornell University, Ithaca, NY 14853, USA. ⁶Clinical Programs Center, College of Veterinary Medicine, Cornell University, Box 31, Ithaca, NY 14853, USA. ⁷These authors contributed equally: Santiago Peralta and Jennifer K. Grenier. ✉email: sp888@cornell.edu

higher in multi-cat compared to single-cat environments and correlates with the number of cohabiting cats¹⁸, suggesting that infectious agents and/or social and hierarchical interactions that could result in chronic stress and immunosuppression could be involved in pathogenesis. Interestingly, numerous studies have shown that most cats with FCGS chronically shed feline calicivirus (FCV)^{19–23}, which aligns with the reported prevalence patterns of FCGS^{18,24}, but a causative role has yet to be demonstrated.

Possible environmental triggers aside, studies have attempted to characterize the abnormal immune response in cats with FCGS both at a local and systemic level. Targeted studies^{25–27} of affected tissues have revealed cytokine expression patterns consistent with a mixed local Th1 and Th2 response and upregulation of *TLR2* and *TLR7*, suggesting signaling due to antigenic stimulation. One transcriptomic study⁷ in three cats that were refractory to surgery showed gene expression patterns consistent with an inflammatory response driven by cytokines. Immunophenotyping assays showed that affected tissues are primarily infiltrated by B cells and CD4+ and CD8+ T cells, and that affected cats have relatively high levels of circulating activated CD8+ T cells⁷, and an underlying viral etiology was speculated. Although interesting, these targeted observations provide limited biological insights given their restricted phenotypes and/or small sample sizes examined. Unsurprisingly, the mechanisms governing disease initiation and progression remain largely unknown, and molecular events that could be clinically targeted have yet to be identified. Therefore, the aim of this study was to generate a transcriptomic dataset that allows unbiased comparative analyses of the local immune response in a relatively large cohort of cats with FCGS using healthy animals as controls, as well as animals with periodontitis (PER), to identify candidate genes and pathways involved specifically in the pathogenesis of FCGS that might inform potentially useful biomarkers and therapeutic targets.

Results

Clinical samples. Biological samples obtained from 34 domestic cats were included in this study (Table 1), representing 20 animals clinically diagnosed with FCGS, 6 diagnosed with moderate or severe PER but not FCGS, and 8 animals serving as controls for RNA-seq, immunohistochemistry (IHC) and in situ hybridization (ISH) experiments. The average age of cats with FCGS and PER was 6.75 ± 3.32 and 7.33 ± 4.27 years ($p = 0.6$, Kruskal–Wallis), respectively. The average body weight of cats with FCGS and PER was 4.49 ± 1.09 and 5.08 ± 0.98 kg ($p = 0.29$, Kruskal–Wallis), respectively. The average age of control animals used for RNA-seq assays was 3.78 ± 1.08 years. Regardless of group assignment, most animals were domestic shorthair (28 cats, 71.8%), followed by Siamese (5 cats, 12.8%), domestic longhair (3 cats, 7.7%), Maine Coon (1 cat, 2.6%); 2 cats (5.1%) were of unknown breed. Of the 34 cats included in the study, tissues from 27 were used for RNA-seq experiments representing 15 FCGS samples, 8 healthy oral mucosal (HOM) samples, 6 PER samples, and 3 healthy gingival (HGIN) samples; and from 15 for IHC and ISH assays, representing 13 FCGS samples, 1 positive control sample and 1 negative control sample. Tissues from some cats were used in more than one assay.

RNA-seq, differential gene expression, cluster analysis and qPCR. We established transcriptomic profiles using bulk RNA-seq on caudal oral mucosal tissues from cats diagnosed with FCGS and gingival tissues from cats diagnosed with PER but not with FCGS, as well as matching tissues from healthy controls. We investigated the RNA-seq data to discover genes dysregulated in FCGS and not (or to a lesser degree) in PER, to distinguish characteristics of FCGS from general inflammation of oral tissues. Of the 19,588 protein-coding genes annotated in *Felis_catus_9.0* (Ensembl release 105), 4,207 genes were differentially expressed ($q < 0.05$) in FCGS when compared to HOM, 748 genes in PER compared HGIN, and 2,891 genes in FCGS when compared to PER (Tables S1–S3). Principal component analysis showed that samples clustered according to clinical phenotype, indicating that the primary global signal in the gene expression profiles distinguished diseased from healthy samples (Fig. 1). Altered expression of 9 biologically relevant genes in FCGS cases was validated with qPCR (Fig. 2).

Functional enrichment analyses. To complement differential gene expression findings and gain functional insights, we conducted Gene Set Enrichment Analysis (GSEA)^{28,29} using the RNA-seq data. When comparing FCGS to HOM, enriched gene sets were predominantly associated with inflammation and the immune response (e.g., NFKB and JAK/STAT) and with cytokine signaling (e.g., IL-6, IFN type I and II, IL-17) (Fig. 3, Tables S4–S6, Figs. S1, S2). Notably, *IL6* was either the top leading-edge gene or was among the top leading-edge genes in most inflammation- and immune-related pathways enriched in FCGS; this observation was also reflected when comparing the expression of cytokines and chemokines in the RNA-seq dataset among the different groups (Fig. 4, Table S7). The expression profiles of FCGS compared to HOM and PER revealed enrichment of immune cells with a predominantly myeloid lineage identity (e.g., macrophages, microglia) led by genes typically expressed by myeloid cells (e.g., *CD14*, *CSFR1*, *CSFR3*, *HCK*, *CYBB*; The Human Protein Atlas, <https://www.proteinatlas.org>)³⁰ (Table S8, Fig. S3).

Non-host RNA-seq reads, immunohistochemistry and in situ hybridization. To determine whether viral genomic sequences were present in analyzed tissues, we mapped RNA-seq reads that did not align with *Felis_catus_9.0* to reference sequences. Results showed sequences mapping to reference genomes of FCV, puma feline foamy virus (PFFV), feline leukemia virus, and feline herpesvirus, among others (Table S9). Of the candidate viruses observed, only FCV and PFFV were significantly more common in cats with FCGS ($p = 0.009$ and 0.029 , respectively, Mann–Whitney test). To determine whether FCV antigen or genome was present in affected tissues, we performed IHC and ISH. Both assays failed to confirm the presence of FCV in any FCGS case ($n = 13$) while results for positive and negative controls were appropriate (Fig. 5).

Case information		Assays performed		FCV results						
Case no	Sex	Age (years)	Breed	Body weight (kg)	Phenotype	RNA-seq	FCV IHC and ISH	RNA-seq reads mapping to FCV	FCV IHC	FCV ISH
1	FS	8	DLH	2.9	FCGS	NO	YES	NA	NEG	NEG
2	MN	8	DSH	4.3	FCGS	NO	YES	NA	NEG	NEG
3	MN	7	DSH	5.9	FCGS	NO	YES	NA	NEG	NEG
4	FS	7	DLH	3.5	FCGS	YES*	NO	NO	NA	NA
5	MN	8	DSH	5	FCGS	YES	YES	YES	NEG	NEG
6	FS	9	Maine Coon	4	FCGS	NO	YES	NA	NEG	NEG
7	MN	12	DSH	4.6	FCGS	NO	YES	NA	NEG	NEG
8	FS	9	DSH	3.5	FCGS	YES	YES	NO	NEG	NEG
9	MN	3	DSH	5.1	FCGS	YES*	NO	YES	NA	NA
10	MN	11	DLH	4.9	FCGS	YES	YES	YES	NEG	NEG
11	MN	2	DSH	5	FCGS	YES	NO	YES	NA	NA
12	FS	3	DSH	3.5	FCGS	YES	YES	NO	NEG	NEG
13	FS	8	DSH	3.4	FCGS	YES*	YES	NO	NEG	NEG
14	MN	2	DSH	5.1	FCGS	YES	YES	YES	NEG	NEG
15	FS	11	DSH	3.4	FCGS	YES	NO	NO	NA	NA
16	FS	2	DSH	4.1	FCGS	YES	NO	NO	NA	NA
17	FS	4	DSH	7.6	FCGS	YES	YES	YES	NEG	NEG
18	FS	8	DSH	3.8	FCGS	YES	YES	YES	NEG	NEG
19	MN	10	DSH	5	FCGS	YES	NO	YES	NA	NA
20	MN	3	DSH	5.3	FCGS	YES	NO	YES	NA	NA
21	FS	5	DSH	5.1	HOM	YES (2)	NO	NO	NA	NA
23	F	1	Siamese	3	HOM	YES (2)	NO	NO	NA	NA
24	M	1	DSH	2.8	HOM	YES (2)	NO	NO	NA	NA
22	M	1	Siamese	4.2	HOM/HGIN	YES (2)	NO	NO	NA	NA
25	M	1	DSH	UNK	HOM/HGIN	YES (2)	NO	NO	NA	NA
26	M	1	DSH	UNK	HGIN	YES	NO	NO	NA	NA
28	FS	11	DSH	4.6	PER	YES	NO	NO	NA	NA
29	FS	3	DSH	4.5	PER	YES	NO	YES	NA	NA
30	MN	3	DSH	7	PER	YES	NO	NO	NA	NA
31	MN	5	Siamese	4.6	PER	YES	NO	NO	NA	NA
32	MN	9	DSH	4.5	PER	YES	NO	NO	NA	NA
33	MN	13	DSH	5.3	PER	YES	NO	NO	NA	NA
27	UNK	UNK	UNK	UNK	FCV negative control	NO	YES	NA	NEG	NEG
34	UNK	UNK	UNK	UNK	FCV positive control	NO	YES	NA	POS	POS

Table 1. Case description and assays performed. *FCV* Feline Calicivirus, *IHC* immunohistochemistry, *ISH* in situ hybridization, *FS* female spayed, *MN* male neutered, *F* female, *M* male, *UNK* unknown, *DSH* domestic shorthair, *DLH* domestic longhair, *FCGS* feline chronic gingivostomatitis, *HOM* healthy oral mucosa, *HGIN* healthy gingiva, *PER* periodontitis, *NA* not applicable, *NEG* negative, *POS* positive. *Excluded from gene expression analysis.

Discussion

Despite its clinical relevance, the etiopathogenesis of FCGS remains unresolved. In this study, we performed bulk RNA-seq molecular profiling of affected tissues derived from a cohort of client-owned cats with FCGS and used tissues from cats with PER and unaffected tissues as comparative sets, to identify candidate genes and pathways that can help guide future exploration of novel clinical solutions for FCGS. We complemented transcriptomic findings with IHC and ISH assays to better understand the biological significance of the data and performed RNA-seq validation of biologically relevant differentially expressed genes using qPCR assays to demonstrate technical reproducibility.

Overall, the transcriptional profiles of FCGS tissues were largely dominated by immune- and inflammation-related genes and signaling pathways including NF κ B, JAK/STAT and IFN type I and II signaling, indicating that FCGS is an inflammatory disease potentially related to antigenic stimulation^{6,31,32}. As was expected, cluster analysis showed that all samples segregated according to group assignment, indicating that FCGS and PER have distinct molecular phenotypes. Additionally, there were general similarities in the expression patterns of FCGS when compared to those previously reported in three cats that were refractory to surgical therapy⁷, suggesting

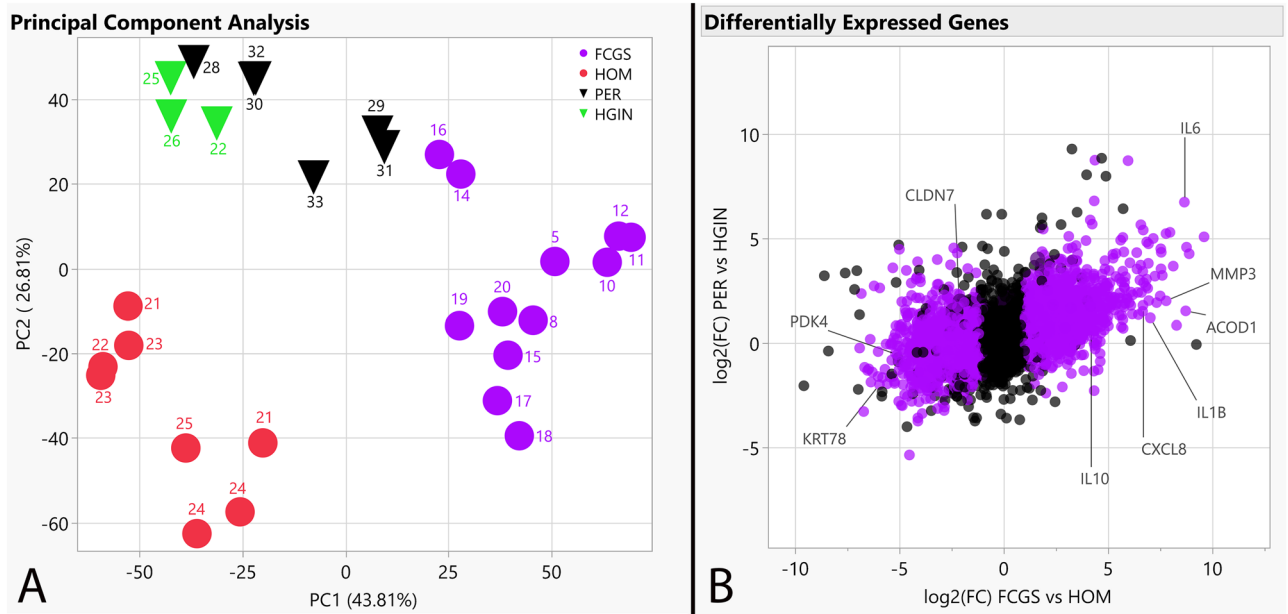


Figure 1. Cluster analysis and differentially expressed genes. **(A)** PCA plot depicting clustering of RNA-seq gene expression profiles showing grouping based on assigned phenotypes and tissue type according to principal components 1 and 2; reverse triangles correspond to gingival samples, dots correspond to caudal oral mucosal samples, labels indicate case numbers as listed in Table 1. **(B)** Scatterplot depicting expressed genes based on $\log_2(\text{FC})$ of affected vs control samples for each disease, with purple points indicating differential expression in FCGS vs PER; genes used for qPCR validation experiments are labeled.

that the molecular mechanisms underlying FCGS are maintained during the natural course of the disease as long as local tissue inflammation persists and regardless of historical surgical interventions.

Notably, most inflammation-related pathways found to be enriched in FCGS tissues appeared to be heavily influenced by *IL6*. This is a relevant finding given that dysregulated expression of IL-6 (encoded by *IL6*) could underlie some of the local and systemic events known to occur in cats with FCGS. In general, IL-6 is a finely regulated pleiotropic cytokine that signals via the JAK/STAT pathway. IL-6 can be produced by multiple cell types including mesenchymal, endothelial, epithelial, and immune cells^{33–35}. During homeostasis, IL-6 blood levels are hardly detectable but can rapidly increase upon stress, tissue injury or antigenic stimulation. Once in circulation, IL-6 activates hepatocytes to produce acute-phase proteins and modulates innate and adaptive immunity to promote healing and help eliminate infections^{36,37}.

Sustained overexpression of IL-6 has been shown to promote chronic inflammation and increase susceptibility to viral infections^{33,35,37,38}. It is possible that excessive production of IL-6 in cats with FCGS explains the chronic FCV and PPFV infection and elevated globulin and acute-phase protein levels in blood typically found, and may be directly involved in perpetuation of oral mucosal inflammation and ulceration. Similarly, IL-6 signaling is a known inhibitor of apoptosis^{39,40}, which might explain the often proliferative nature of mucosal lesions observed in cats with FCGS. Interestingly, recombinant feline IFN-omega has been shown to reduce *IL6* expression and IL-6 levels⁴¹, which could at least partially explain the clinical response reported in some cats with FCGS^{14,15}.

Another interesting finding in FCGS tissues in agreement with a previous report⁷ was overexpression of *IL17A* and enrichment of its corresponding signaling pathway. Importantly, IL-17 (encoded by *IL17A*) is considered the signature cytokine of Th17 cells⁴². Although Th17 cells play an important protective role against microbial and viral pathogens, they are also implicated in autoinflammatory and autoimmune pathology^{42–45}. IL-6 promotes polarization of naïve CD4+ T cells towards a Th17 phenotype^{33,35,36}, thus the increased *IL17A* activity observed in FCGS tissues may be due to IL-6 signaling. However, the cellular origin and biological impact of *IL17A* overexpression in FCGS, and whether activation of the IL-17 pathway plays a pathogenic or protective role in affected cats is unknown but warrants further investigation.

Coinciding with previous reports^{19–23}, this study showed an association between FCGS and FCV and PPFV infection. However, the very low numbers of RNA-seq reads mapping to corresponding viral genomes in affected tissues, and the fact that IHC and ISH failed to detect FCV antigen and genome signals, respectively, suggest that at least FCV does not replicate in areas of mucosal ulceration, or that it is present in such low numbers that it is undetectable using the IHC and ISH techniques used in this study. Regardless, the consistent overexpression of *IFNG*, which encodes IFN-gamma, and enrichment of IFN type I and II pathways suggest an immune response to viral stimulation^{46,47}. Given that *IFNG* induces expression of *CXCL9*, *CXCL10*, and other chemotactic molecules⁴⁸, IFN-gamma signaling is likely to play an important role in immune cell traffic in affected oral mucosal tissues, including attraction of T and B cells. Taken together, these observations implicate viral infection as a possibly required or aggravating element in the pathogenesis of FCGS.

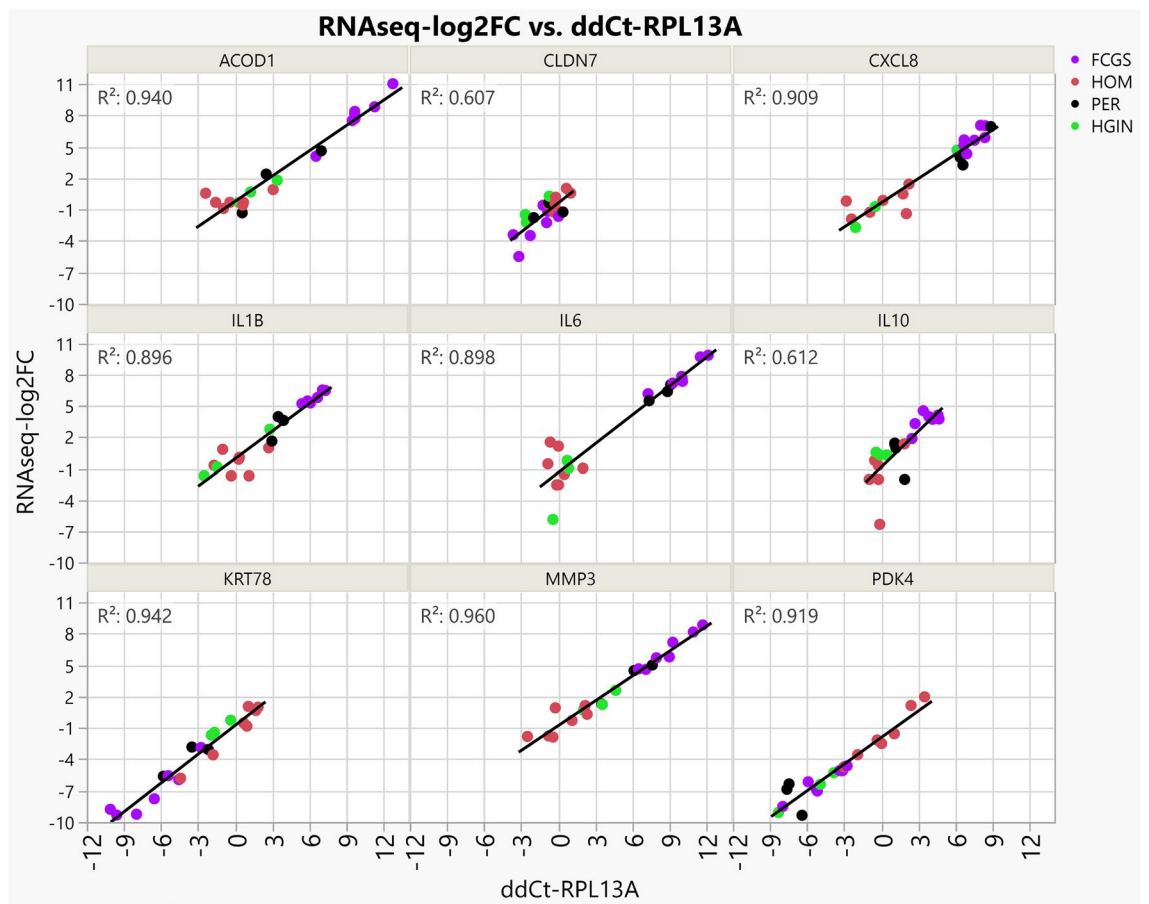


Figure 2. Technical validation of RNA-seq data using qPCR experiments. Scatterplots of qPCR assays (ddCt-RPL13A, X axis) of 9 genes plotted against the results of RNA-seq (RNAseq-log2FC, Y axis), where RNAseq-log2FC is the difference between the log2 normalized expression for each sample compared to the average log2 normalized expression for healthy control samples. The measurements with both gene expression quantification platforms were in excellent agreement for all phenotypes.

Unexpectedly, the gene expression signatures observed in FCGS tissues revealed a predominantly myeloid lineage identity, which suggests that despite the heavy presence of lymphoid infiltrates, the innate system is transcriptionally more active and is thus likely to be an important driver of the dysregulated immune response. This finding conflicts with the hypothesis that FCGS is primarily a T cell driven disease⁷. As macrophages and monocytes are the main producers of IL-6^{34,35}, these new findings support a hypothesis that IL-6 dysregulation underlies some of the pathological events. Regardless, it would be interesting to determine if the typical plasma cell infiltrates correspond to pathogenic memory plasma cells, and how these might contribute to disease. Similarly, whether immune regulatory mechanisms are involved in pathogenesis should be investigated, especially given that *FOXP3* appeared differentially upregulated in FCGS tissues.

The caudal oral mucosa of cats is a relatively thin, non-masticatory mucosal barrier that is exposed to mechanical trauma during mastication, and to pathogenic toxins (e.g., LPS) derived from the oral microbiota⁴⁹. Given this environment, it is possible that the caudal oral mucosa is particularly susceptible to immune stimulation, and that in some cases such stimuli result in chronic inflammation. This could explain why extraction of premolar and molar teeth, which typically come in direct contact with caudal and buccal oral mucosal surfaces, results in remission in some animals^{9,10}. Alternatively or in addition, based on the transcriptional signatures observed in this study and the epidemiological patterns previously reported¹⁸, it is possible that viruses and environmental stressors are involved in the pathogenesis of FCGS; both are likely to contribute to upregulation of IL-6⁴⁹. Such a scenario raises the question of why, when subject to similar conditions (i.e., multi-cat environments), only some individuals develop FCGS. Possible explanations could include unknown exposures and/or genetic or epigenetic predisposition.

From a translational medicine perspective, the results of this study provide rational targets for clinical diagnostics and therapy in cats with FCGS. For example, IL-6 could be investigated as a potential diagnostic and prognostic marker that could be used to stage and grade FCGS, determine the best treatment modalities or predict therapeutic response. Similarly, given the precedent of successful targeted inhibition of IL-6 signaling in people diagnosed with certain chronic inflammatory conditions and different forms of cancer^{33,34,36,40}, comparable approaches could be tested in cats with FCGS. It should be noted that the expression signatures reported

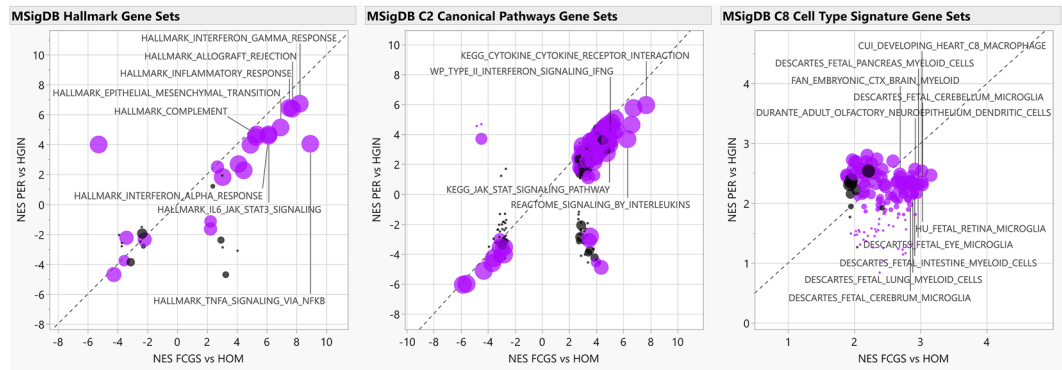


Figure 3. Functional enrichment analyses. The scatterplots depict normalized enrichment scores (NES) as calculated by GSEA, for represented gene sets from MSigDB for analyses of FCGS vs HOM (i.e., FDR q -value < 0.05 , X axis) and comparison to PER vs HGIN (Y axis). Gene sets differentially enriched or depleted (i.e., FDR q -value < 0.05) in FCGS compared to PER appear in purple. For all graphs, relevant gene sets and pathways are labeled. The size of the dots is based on $-\log_{10}$ transformed p -values based on enrichment scores comparison of FCGS vs PER.

here capture global trends, but further studies are required to determine their biological impact. Importantly, bulk RNA-seq techniques using clinical samples do not allow single-cell inferences or insights of how different cell types interact with each other. Therefore, the observations made here represent hypotheses that will require testing using targeted, single-cell and/or spatially resolved approaches, and ideally in vitro and in vivo validation experiments.

We conclude that the transcriptomic profile of oral mucosal tissues in cats with FCGS is enriched with immune- and inflammation-related genes and pathways that appear to be largely influenced by *IL6*, and include NFKB, JAK/STAT, IL-17 and IFN type I and II signaling.

Materials and methods

Clinical samples. Study material consisted of cryopreserved and formalin-fixed paraffin-embedded (FFPE) oral mucosal and gingival tissues and cryopreserved serum samples obtained from cats presented to the Dentistry and Oral Surgery Service at the Cornell University Hospital for Animals (FCGS and PER tissues), and archival tissues stored in the Cornell Veterinary Biobank (HOM and HGIN tissues). Clinical sample collection procedures were performed in accordance with a protocol (#2005-0151) approved by Cornell University's Institutional Animal Care and Use Committee while animals were receiving standard-of-care intervention under general anesthesia, which was supervised by a board-certified veterinary anesthesiologist following standard-of-care clinical practices and protocols, as determined by individual patient needs. Informed consent to authorize the use of tissue samples and clinical data for research purposes was obtained from cat owners prior to sample collection, and undue harm was never inflicted to any animal for the purposes of this study; all methods were performed in accordance with the relevant guidelines and regulations as approved in the protocol previously listed. Clinical diagnoses and sample collection were supervised by a board-certified veterinary dentistry specialist (SP). None of the FCGS cats enrolled had been previously treated by surgical means or were considered refractory to therapy at the time of sampling. Control tissue samples were collected from healthy cats, including replicate oral mucosal samples from two separate locations from 3 cats. Age and weight differences across groups were compared using JMP 15 (SAS Institute Inc., Cary, NC); box plots were generated using BoxPlotR (<http://shiny.chemgrid.org/boxplotr/>)⁵⁰.

RNA isolation, library preparation and sequencing. Frozen tissue (~1 g) was homogenized in 2 mL of Trizol (Thermo Fisher) using 2.8 mm ceramic beads (Hard Tissue Homogenizing Mix, VWR). RNA was extracted with a modified Trizol method as follows: after the addition of chloroform and phase separation of the Trizol lysate, the aqueous phase was combined with an equal volume of 100% ethanol and loaded onto a Zymo-Spin column and purified using the Quick-RNA Prep Kit (Zymo Research). For all samples, RNA concentration was measured with a Nanodrop (Thermo Fisher), and integrity was determined with a Fragment Analyzer (Agilent). If high molecular weight material was evident in the Fragment Analyzer trace, indicating the presence of genomic DNA, samples were treated with DNase following the instructions of the Zymo RNA Clean & Concentrator Kit (Zymo Research). Ribosomal RNA was depleted with the NEBNext rRNA Depletion Kit v2 (Human/Mouse/Rat; New England Biolabs) using 500 ng input total RNA. All RNA-seq libraries were generated with the NEBNext Ultra II Directional library prep kit (New England Biolabs) and 2×150 nt paired-end reads were generated on a NovaSeq6000 instrument (Illumina).

RNA-seq Analysis. Raw reads were trimmed for low-quality and adaptor sequences and filtered for minimum length with TrimGalore (http://www.bioinformatics.babraham.ac.uk/projects/trim_galore/), a wrapper for cutadapt⁵¹ and fastQC (<http://www.bioinformatics.babraham.ac.uk/projects/fastqc/>) using

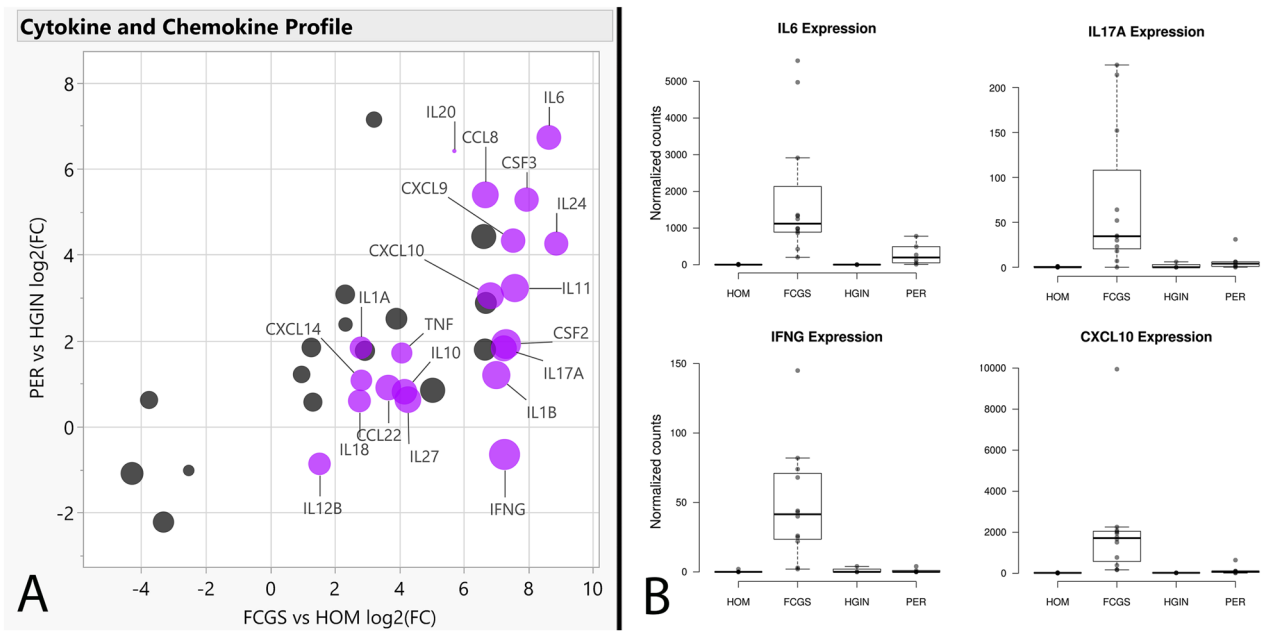


Figure 4. Cytokine and chemokine expression profiles. (Panel A) shows a scatterplot depicting log₂(FC) values of FC GS vs HOM (X axis) and PER vs HGIN (Y axis), with genes significantly enriched in FC GS vs PER shown in purple. The size of the dots is based on log₂(FC) of FC GS vs PER. (Panel B) shows box plots depicting the normalized counts distribution for *IL6*, *IL17A*, *IFNG*, and *CXCL10* according to phenotype.

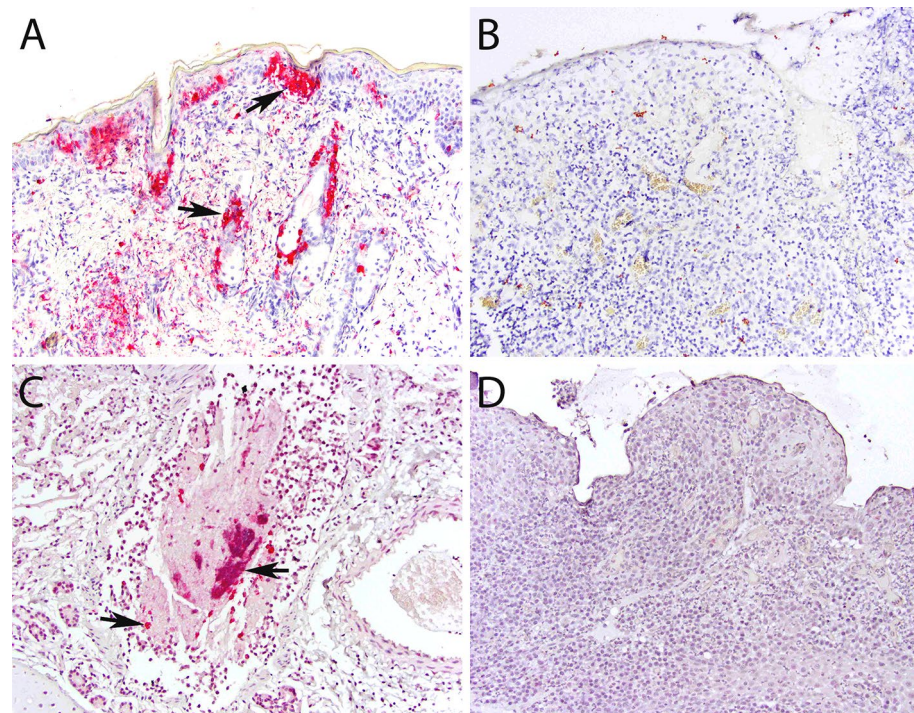


Figure 5. Immunohistochemistry and in situ hybridization results. (A) (IHC, skin, FCV-infected cat, ×200 magnification): positive control; strong immunolabeling in epidermal and adnexal epithelial cells (arrows) and dermal leukocytes and/or mesenchymal cells. (B) (IHC, oral mucosa, FC GS-affected cat, ×200 magnification): no cells are immunolabeled. (C) (ISH, lungs, FCV-infected cat, ×200 magnification): positive control; strong signal in leukocytes, epithelial cells, and debris within the bronchiolar lumen. (D) (ISH, oral mucosa, FC GS-affected cat, ×200 magnification): no signal is identified.

parameters ‘-nextseq-trim=20 -O 1 -a AGATCGGAAGAGC -length 50 -fastqc’. Trimmed reads were mapped to the reference genome/transcriptome (Ensembl felCat9) with STAR⁵² using these parameters: ‘-outSAMstrandField intronMotif, -outFilterIntronMotifs RemoveNoncanonical, -outSAMtype BAM SortedByCoordinate, -outReadsUnmapped Fastx and -quantMode GeneCounts’, which also generated raw count outputs per annotated gene. Samples with low rates of reads mapping to the FelCat9 reference genome or transcriptome were excluded from gene expression analysis, including three FCGS cases for which the reads were still analyzed for evidence of feline viruses (cases 4, 9, 13).

Sample clustering and differential gene expression were analyzed with SARTools⁵³ and DESeq2⁵⁴ using these parameters: ‘fitType parametric, cooksCutoff TRUE, independentFiltering TRUE, alpha 0.05, pAdjustMethod BH, typeTrans VST, and locfunc median’. Feline gene symbols were converted to human gene symbols using Biomart (Ensembl) one-to-one orthology assignments to enable analysis with gene sets in MSigDB²⁸. The human ortholog gene symbols and log₂-fold-change values for expressed genes (at least one group with average normalized counts > 50) were used for GSEA²⁹ ‘Preranked’ analysis.

Reads that did not map to the feline reference genome were defined as non-host and separately analyzed for evidence of viral infection. Non-host reads were mapped to the RefSeq sequence for candidate feline virus genomes using bowtie2 using local alignment settings (-local). Counts per million (CPM) was calculated as the number of mapped reads per million non-host reads, and p-values were determined comparing FCGS vs HOM samples with the Mann Whitney test (<https://astatsa.com/WilcoxonTest>, default parameters).

qPCR validation. Gene expression levels were validated using real-time reverse transcription polymerase chain reaction (qPCR). Genes were selected for validation based on several criteria, including biological relevance to the disease state (e.g., interleukins and chemokines, immunometabolism), evidence for differential expression of gene families (e.g., metalloproteinases, keratins, claudins), level of detection in the RNA-seq dataset, and altered expression in a majority FCGS cases. cDNA was synthesized as previously described^{55,56}. All cDNA reactions were diluted 20-fold with water prior to qPCR reaction setup. Primer pairs (Table 2) were designed with Primer-BLAST (NCBI), separated by an intron to minimize amplification of residual contaminating genomic DNA and allow identification of alternate amplicons with melt curve analysis. RPL13A was selected as the endogenous control gene, as this gene showed minimal variation across samples in the RNA-seq data. Each primer pair was validated using a standard curve of six four-fold serial dilutions of a representative sample of pooled cDNA. A ‘No-RT’ control containing RNA but lacking M-MuLV enzyme and one ‘no template’ control lacking any cDNA sample was included for each primer pair standard curve validation. Primer pairs that did not generate signal in < 35 cycles or that exhibited non-quantitative performance (i.e., < > 2-cycle shifts for fourfold dilution series), non-specific signal in negative controls, or variable amplicon identities as determined by melt curve analysis were excluded. All primer pairs passed validation by standard curve testing. Each qPCR reaction was prepared in 8 µL reaction volumes in an optically clear 384-well PCR plate with seal using the Luna Universal qPCR Master Mix (New England Biolabs) with 0.25 µM primers and 4 µL pre-diluted sample cDNA. All reactions were performed in triplicate using a Roche LightCycler 480 instrument. Cycles were as follows: initial incubation 5 min at 95 °C; followed by 45 cycles of 30 s at 95 °C; 30 s at 60 °C; 10 s at 72 °C with data acquisition; and final a melt curve with a ramp from 60 to 95 °C at 2 °C per second. Melt curve analysis was used to identify and exclude reactions with alternative amplicons. For relative quantification estimates for each target gene, the $\Delta\Delta Ct$ value [$\Delta Ct_{SAMPLE} - \Delta Ct_{REF}$] was calculated for each sample, where ΔCt_{SAMPLE} = average (target gene Ct) – average (all endogenous control Ct) and ΔCt_{REF} was defined as the average ΔCt_{SAMPLE} for the normal samples. The normalized relative amount of the target gene is $2^{-\Delta\Delta Ct}$ ⁷⁷.

Immunohistochemistry and in situ hybridization assays. For IHC, selected FFPE tissue blocks were processed for antigen retrieval and detection by using an automated IHC processor (Leica Bond-Max, Leica Biosystems, Buffalo Grove, Illinois, USA), as previously described⁵⁷. Briefly, sections were dewaxed (cat# AR9222, Bond Dewax Solution, Leica) and processed for epitope retrieval (cat# AR9961 or AR9640, Bond Epitope Retrieval solution, Leica) followed by incubation with an FCV primary antibody (ABCAM Cat#

Target feline gene	Forward (5' → 3')	Reverse (5' → 3')	Product (bp)
ACOD1	CACTCCTGAGATAAGCCTCCTC	TCTGGCAAAGCTTTCTGTGAC	65
CLDN7	TGAATCTGAAGTACGAGTTCGGTCC	CTCCCGGACAGGAGCAAG	103
CXCL8	TTTCTGCAGCTCTGTGTGAAGC	CAGTGTGGGCCACTGTCAATC	139
IL1B	GAACCAACAAGTGGTGTCCG	TCCCGTCTTTCATCACACAGG	122
IL6	ACACCAAGTACTAACGTCCTGC	CTTCTACGGTTGGGACAGGG	87
IL10	TCAAACAGCAGTGAACCTCC	AGGTACTCTTACCTGTCTCCAC	123
KRT78	CAGCTCCAGAGAGAACAAGGG	GTCATTCTCAAGTGTGGCGTG	120
MMP3	AGGACAAATACTGGCGATTGATG	GCGAAGAGCCACTGAAGAAATAG	150
PDK4	TTCCAGGCCAGCCAATTCAC	TCCTGGTGTCAACTGTCCG	103
RPL13A*	ACAGAAACAAGTTGAAGTACTTGGC	CATGCCTCGCACCGTCC	119

Table 2. Primer pairs used for qPCR. Genes, primer pairs, and product size (bp = base pairs) used for qPCR analysis. *Endogenous control gene.

AB33990) at a 1:200 dilution for 60 min. Next, polymeric alkaline phosphatase conjugated anti-mouse IgG (cat# PV6110, Powervision™ Poly-AP Anti-Mouse IgG, Leica) was applied for 30 min, followed by Red Detection™ (cat# DS9390, Bond Refine Red Detection Kit, Leica) for 15 min, and hematoxylin counterstain for 5 min. Archival FCV-infected and non-infected tissues were used as positive and negative controls.

The same selected FFPE tissues used for IHC were used for ISH. Probes were designed in collaboration with Advanced Cell Diagnostics (ACD, Cat. No. 472281). Briefly, 5- μ m sections were cut and stored at -80°C prior to staining. Sections were deparaffinized in xylene, washed with ethanol, and dried. Staining was performed according to the manufacturer's protocol for colorimetric ISH. Slides were treated with H_2O_2 (ACD) to block endogenous peroxidases for 10 min. Slides were antigen-retrieved by boiling for 15 min in antigen retrieval solution (ACD) and then treated with proteinase K (ACD) for 30 min. Slides were then incubated for 2 h with FCV probes, and then 6 amplification steps were performed with ACD reagents. The bacterial gene DapB probe (ACD) was used as a negative control. Slides were developed with DAB chromogen (ACD) for 10 min and counterstained with Mayer's hematoxylin (Dako). Archival FCV-infected and non-infected tissues were used as positive and negative controls.

Data availability

The gene expression data is available at the NCBI Gene Expression Omnibus (GEO) with accession number GSE230491.

Received: 23 April 2023; Accepted: 16 August 2023

Published online: 18 August 2023

References

- Lee, D. B., Verstraete, F. J. M. & Arzi, B. An update on feline chronic gingivostomatitis. *Vet. Clin. North Am. Small Anim. Pract.* **50**, 973–982. <https://doi.org/10.1016/j.cvsm.2020.04.002> (2020).
- Lyon, K. F. Gingivostomatitis. *Vet. Clin. North Am. Small Anim. Pract.* **35**, 891–911. <https://doi.org/10.1016/j.cvsm.2005.02.001> (2005).
- Farcas, N., Lommer, M. J., Kass, P. H. & Verstraete, F. J. Dental radiographic findings in cats with chronic gingivostomatitis (2002–2012). *J. Am. Vet. Med. Assoc.* **244**, 339–345. <https://doi.org/10.2460/javma.244.3.339> (2014).
- Rodrigues, M. X., Bicalho, R. C., Fiani, N., Lima, S. F. & Peralta, S. The subgingival microbial community of feline periodontitis and gingivostomatitis: Characterization and comparison between diseased and healthy cats. *Sci. Rep.* **9**, 12340. <https://doi.org/10.1038/s41598-019-48852-4> (2019).
- Rodrigues, M. X., Fiani, N., Bicalho, R. C. & Peralta, S. Preliminary functional analysis of the subgingival microbiota of cats with periodontitis and feline chronic gingivostomatitis. *Sci. Rep.* **11**, 6896. <https://doi.org/10.1038/s41598-021-86466-x> (2021).
- Harley, R., Gruffydd-Jones, T. J. & Day, M. J. Salivary and serum immunoglobulin levels in cats with chronic gingivostomatitis. *Vet. Rec.* **152**, 125–129 (2003).
- Vapniarsky, N. *et al.* Histological, immunological, and genetic analysis of feline chronic gingivostomatitis. *Front. Vet. Sci.* <https://doi.org/10.3389/fvets.2020.00310> (2020).
- Winer, J. N., Arzi, B. & Verstraete, F. J. M. Therapeutic management of feline chronic gingivostomatitis: A systematic review of the literature. *Front. Vet. Sci.* **3**, 54. <https://doi.org/10.3389/fvets.2016.00054> (2016).
- Hennet, P. Chronic gingivo-stomatitis in cats: Long-term follow-up of 30 cases treated by dental extractions. *J. Vet. Dent.* **14**, 15–21 (1997).
- Jennings, M. W., Lewis, J. R., Soltero-Rivera, M. M., Brown, D. C. & Reiter, A. M. Effect of tooth extraction on stomatitis in cats: 95 cases (2000–2013). *J. Am. Vet. Med. Assoc.* **246**, 654–660. <https://doi.org/10.2460/javma.246.6.654> (2015).
- Lommer, M. J. Efficacy of cyclosporine for chronic, refractory stomatitis in cats: A randomized, placebo-controlled, double-blinded clinical study. *J. Vet. Dent.* **30**, 8–17. <https://doi.org/10.1177/089875641303000101> (2013).
- Arzi, B. *et al.* Therapeutic efficacy of fresh, autologous mesenchymal stem cells for severe refractory gingivostomatitis in cats. *Stem Cells Transl. Med.* **5**, 75–86. <https://doi.org/10.5966/sctm.2015-0127> (2016).
- Arzi, B. *et al.* A multicenter experience using adipose-derived mesenchymal stem cell therapy for cats with chronic, non-responsive gingivostomatitis. *Stem Cell Res. Ther.* **11**, 1–13 (2020).
- Li, S. F. *et al.* Interferon-omega: Current status in clinical applications. *Int. Immunopharmacol.* **52**, 253–260. <https://doi.org/10.1016/j.intimp.2017.08.028> (2017).
- Hennet, P. R., Camy, G. A., McGahie, D. M. & Albouy, M. V. Comparative efficacy of a recombinant feline interferon omega in refractory cases of calicivirus-positive cats with caudal stomatitis: A randomised, multi-centre, controlled, double-blind study in 39 cats. *J. Feline Med. Surg.* **13**, 577–587. <https://doi.org/10.1016/j.jfms.2011.05.012> (2011).
- Healey, K. A. *et al.* Prevalence of feline chronic gingivo-stomatitis in first opinion veterinary practice. *J. Feline Med. Surg.* **9**, 373–381. <https://doi.org/10.1016/j.jfms.2007.03.003> (2007).
- Verhaert, L. & Van Wetter, C. Survey of oral diseases in cats in Flanders. *Vlaams diergeneeskundig tijdschrift* **73**, 331–340 (2004).
- Peralta, S. & Carney, P. C. Feline chronic gingivostomatitis is more prevalent in shared households and its risk correlates with the number of cohabiting cats. *J. Feline Med. Surg.* <https://doi.org/10.1177/1098612x18823584> (2019).
- Knowles, J. O., Gaskell, R. M., Gaskell, C. J., Harvey, C. E. & Lutz, H. Prevalence of feline calicivirus, feline leukaemia virus and antibodies to FIV in cats with chronic stomatitis. *Vet. Rec.* **124**, 336–338 (1989).
- Knowles, J. O. *et al.* Studies on the role of feline calicivirus in chronic stomatitis in cats. *Vet. Microbiol.* **27**, 205–219 (1991).
- Lommer, M. J. & Verstraete, F. J. Concurrent oral shedding of feline calicivirus and feline herpesvirus 1 in cats with chronic gingivostomatitis. *Oral Microbiol. Immunol.* **18**, 131–134 (2003).
- Druet, I. & Hennet, P. Relationship between Feline calicivirus Load, Oral Lesions, and Outcome in Feline Chronic Gingivostomatitis (Caudal Stomatitis): Retrospective Study in 104 Cats. *Front. Vet. Sci.* **4**, 209. <https://doi.org/10.3389/fvets.2017.00209> (2017).
- Fried, W. A. *et al.* Use of unbiased metagenomic and transcriptomic analyses to investigate the association between feline calicivirus and feline chronic gingivostomatitis in domestic cats. *Am. J. Vet. Res.* **82**, 381–394. <https://doi.org/10.2460/ajvr.82.5.381> (2021).
- Pesavento, P. A., Chang, K. O. & Parker, J. S. Molecular virology of feline calicivirus. *Vet. Clin. North Am. Small Anim. Pract.* **38**, 775–786. <https://doi.org/10.1016/j.cvsm.2008.03.002> (2008).
- Harley, R., Helps, C. R., Harbour, D. A., Gruffydd-Jones, T. J. & Day, M. J. Cytokine mRNA expression in lesions in cats with chronic gingivostomatitis. *Clin. Diagn. Lab. Immunol.* **6**, 471–478 (1999).
- Dolieslager, S. M., Bennett, D., Johnston, N. & Riggio, M. P. Novel bacterial phylotypes associated with the healthy feline oral cavity and feline chronic gingivostomatitis. *Res. Vet. Sci.* **94**, 428–432. <https://doi.org/10.1016/j.rvsc.2012.11.003> (2013).

27. Dolieslager, S. M. *et al.* The influence of oral bacteria on tissue levels of Toll-like receptor and cytokine mRNAs in feline chronic gingivostomatitis and oral health. *Vet. Immunol. Immunopathol.* **151**, 263–274. <https://doi.org/10.1016/j.vetimm.2012.11.016> (2013).
28. Liberzon, A. *et al.* Molecular signatures database (MSigDB) 3.0. *Bioinformatics* **27**, 1739–1740. <https://doi.org/10.1093/bioinformatics/btr260> (2011).
29. Subramanian, A. *et al.* Gene set enrichment analysis: A knowledge-based approach for interpreting genome-wide expression profiles. *Proc. Natl. Acad. Sci. U.S.A.* **102**, 15545–15550. <https://doi.org/10.1073/pnas.0506580102> (2005).
30. Pontén, F., Jirstrom, K. & Uhlen, M. The human protein atlas—a tool for pathology. *J. Pathol.* **216**, 387–393. <https://doi.org/10.1002/path.2440> (2008).
31. Arzi, B. *et al.* Analysis of immune cells within the healthy oral mucosa of specific pathogen-free cats. *Anat. Histol. Embryol.* **40**, 1–10. <https://doi.org/10.1111/j.1439-0264.2010.01031.x> (2011).
32. Harley, R., Gruffydd-Jones, T. J. & Day, M. J. Immunohistochemical characterization of oral mucosal lesions in cats with chronic gingivostomatitis. *J. Comp. Pathol.* **144**, 239–250. <https://doi.org/10.1016/j.jcpa.2010.09.173> (2011).
33. Hirano, T. IL-6 in inflammation, autoimmunity and cancer. *Int. Immunol.* **33**, 127–148. <https://doi.org/10.1093/intimm/dxaa078> (2020).
34. Tanaka, T., Narazaki, M., Masuda, K. & Kishimoto, T. Regulation of IL-6 in immunity and diseases. In *Regulation of Cytokine Gene Expression in Immunity and Diseases* 79–88 (Springer, 2016).
35. Unver, N. & McAllister, F. IL-6 family cytokines: Key inflammatory mediators as biomarkers and potential therapeutic targets. *Cytokine Growth Factor Rev.* **41**, 10–17. <https://doi.org/10.1016/j.cytogfr.2018.04.004> (2018).
36. Chalaris, A., Garbers, C., Rabe, B., Rose-John, S. & Scheller, J. The soluble Interleukin 6 receptor: Generation and role in inflammation and cancer. *Eur. J. Cell Biol.* **90**, 484–494. <https://doi.org/10.1016/j.ejcb.2010.10.007> (2011).
37. Gabay, C. Interleukin-6 and chronic inflammation. *Arthritis Res. Ther.* **8**, S3. <https://doi.org/10.1186/ar1917> (2006).
38. Velazquez-Salinas, L., Verdugo-Rodriguez, A., Rodriguez, L. L. & Borca, M. V. The role of Interleukin 6 during viral infections. *Front. Microbiol.* <https://doi.org/10.3389/fmicb.2019.01057> (2019).
39. Yu, H., Pardoll, D. & Jove, R. STATs in cancer inflammation and immunity: A leading role for STAT3. *Nat. Rev. Cancer* **9**, 798–809. <https://doi.org/10.1038/nrc2734> (2009).
40. Kasembeli, M. M., Bharadwaj, U., Robinson, P. & Tweardy, D. J. Contribution of STAT3 to inflammatory and fibrotic diseases and prospects for its targeting for treatment. *Int. J. Mol. Sci.* **19**, 2299. <https://doi.org/10.3390/ijms19082299> (2018).
41. Leal, R. O. *et al.* Evaluation of viremia, proviral load and cytokine profile in naturally feline immunodeficiency virus infected cats treated with two different protocols of recombinant feline interferon omega. *Res. Vet. Sci.* **99**, 87–95. <https://doi.org/10.1016/j.rvsc.2015.02.008> (2015).
42. Dong, W. & Ma, X. Regulation of Interleukin-17 production. *Adv. Exp. Med. Biol.* **941**, 139–166. https://doi.org/10.1007/978-94-024-0921-5_7 (2016).
43. Deng, J., Yu, X.-Q. & Wang, P.-H. Inflammasome activation and Th17 responses. *Mol. Immunol.* **107**, 142–164 (2019).
44. Peters, A. & Yosef, N. Understanding Th17 cells through systematic genomic analyses. *Curr. Opin. Immunol.* **28**, 42–48. <https://doi.org/10.1016/j.coi.2014.01.017> (2014).
45. Tesmer, L. A., Lundy, S. K., Sarkar, S. & Fox, D. A. Th17 cells in human disease. *Immunol. Rev.* **223**, 87–113. <https://doi.org/10.1111/j.1600-065X.2008.00628.x> (2008).
46. Walter, M. R. The role of structure in the biology of interferon signaling. *Front. Immunol.* **11**, 6489. <https://doi.org/10.3389/fimmu.2020.606489> (2020).
47. Kang, S., Brown, H. M. & Hwang, S. Direct antiviral mechanisms of interferon-gamma. *Immune Netw.* **18**, e33. <https://doi.org/10.4110/in.2018.18.e33> (2018).
48. Marshall, A., Celentano, A., Cirillo, N., McCullough, M. & Porter, S. Tissue-specific regulation of CXCL9/10/11 chemokines in keratinocytes: Implications for oral inflammatory disease. *PLoS ONE* **12**, e0172821. <https://doi.org/10.1371/journal.pone.0172821> (2017).
49. Gaffen, S. L. & Moutsopoulos, N. M. Regulation of host-microbe interactions at oral mucosal barriers by type 17 immunity. *Sci. Immunol.* <https://doi.org/10.1126/sciimmunol.aau4594> (2020).
50. Spitzer, M., Wildenhain, J., Rappsilber, J. & Tyers, M. BoxPlotR: A web tool for generation of box plots. *Nat. Methods* **11**, 121–122. <https://doi.org/10.1038/nmeth.2811> (2014).
51. Martin, M. Cutadapt removes adapter sequences from high-throughput sequencing reads. *EMBnet J* **17**, 10–12 (2011).
52. Dobin, A. *et al.* STAR: Ultrafast universal RNA-seq aligner. *Bioinformatics* **29**, 15–21. <https://doi.org/10.1093/bioinformatics/bts635> (2013).
53. Varet, H., Brillet-Gueguen, L., Coppee, J. Y. & Dillies, M. A. SARTools: A DESeq2- and EdgeR-based R pipeline for comprehensive differential analysis of RNA-seq data. *PLoS One* **11**, e0157022. <https://doi.org/10.1371/journal.pone.0157022> (2016).
54. Love, M. I., Huber, W. & Anders, S. Moderated estimation of fold change and dispersion for RNA-seq data with DESeq2. *Genome Biol.* **15**, 550. <https://doi.org/10.1186/s13059-014-0550-8> (2014).
55. Peralta, S. *et al.* Comparative transcriptional profiling of canine acanthomatous ameloblastoma and homology with human ameloblastoma. *Sci. Rep.* **11**, 17792. <https://doi.org/10.1038/s41598-021-97430-0> (2021).
56. Peralta, S., McCleary-Wheeler, A. L., Duhamel, G. E., Heikinheimo, K. & Grenier, J. K. Ultra-frequent HRAS p.Q61R somatic mutation in canine acanthomatous ameloblastoma reveals pathogenic similarities with human ameloblastoma. *Vet. Comp. Oncol.* **17**, 439–445. <https://doi.org/10.1111/vco.12487> (2019).
57. Peralta, S., Grenier, J. K., McCleary-Wheeler, A. L. & Duhamel, G. E. Ki67 labelling index of neoplastic epithelial cells differentiates canine acanthomatous ameloblastoma from oral squamous cell carcinoma. *J. Comp. Pathol.* **171**, 59–69. <https://doi.org/10.1016/j.jcpa.2019.08.001> (2019).

Acknowledgements

This study was performed using funds kindly provided by the Cornell Feline Health Center and by the Foundation for Veterinary Dentistry. Cryopreserved samples and associated phenotypic data were provided by the Cornell Veterinary Biobank, a resource built with the support of NIH grant R24 GM082910 and the Cornell University College of Veterinary Medicine. Gene expression profiling was conducted by the Transcriptional Regulation and Expression Facility at Cornell University.

Author contributions

S.P., J.K.G., A.D.M., I.C.M., and J.S.L.P. conceived the study; S.P. and J.K.G. analyzed and interpreted genomic data; J.K.G. and S.M.W. designed and performed technical validation of genomic data; A.D.M. and I.C.M. reviewed and interpreted pathology slides; S.P. collected clinical samples and associated data and drafted the manuscript; all authors reviewed, edited, and approved the manuscript.

Competing interests

The authors declare no competing interests.

Additional information

Supplementary Information The online version contains supplementary material available at <https://doi.org/10.1038/s41598-023-40679-4>.

Correspondence and requests for materials should be addressed to S.P.

Reprints and permissions information is available at www.nature.com/reprints.

Publisher's note Springer Nature remains neutral with regard to jurisdictional claims in published maps and institutional affiliations.



Open Access This article is licensed under a Creative Commons Attribution 4.0 International License, which permits use, sharing, adaptation, distribution and reproduction in any medium or format, as long as you give appropriate credit to the original author(s) and the source, provide a link to the Creative Commons licence, and indicate if changes were made. The images or other third party material in this article are included in the article's Creative Commons licence, unless indicated otherwise in a credit line to the material. If material is not included in the article's Creative Commons licence and your intended use is not permitted by statutory regulation or exceeds the permitted use, you will need to obtain permission directly from the copyright holder. To view a copy of this licence, visit <http://creativecommons.org/licenses/by/4.0/>.

© The Author(s) 2023